Formation of Magnetic Structures in Density Stratified Turbulence in Plasma with Large Beta

I. ROGACHEVSKII, N. KLEEORIN,

Ben-Gurion University of the Negev, Beer Sheva, Israel

NORDITA, KTH Royal Institute of Technology and Stockholm University, Sweden

A. BRANDENBURG, S. JABBARI, K. KEMEL, I.R. LOSADA, Dh. MITRA

NORDITA, KTH Royal Institute of Technology and Stockholm University, and Department of Astronomy, Stockholm University, Sweden

J. WARNECKE, P. KÄPYLÄ, M. KORPI-LAGG

Max-Planck-Institut für Sonnesystemforschung, Göttingen, Germany

Aalto University, Espoo, Finland

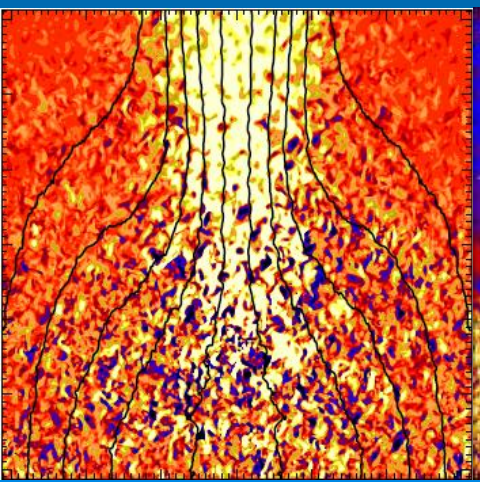

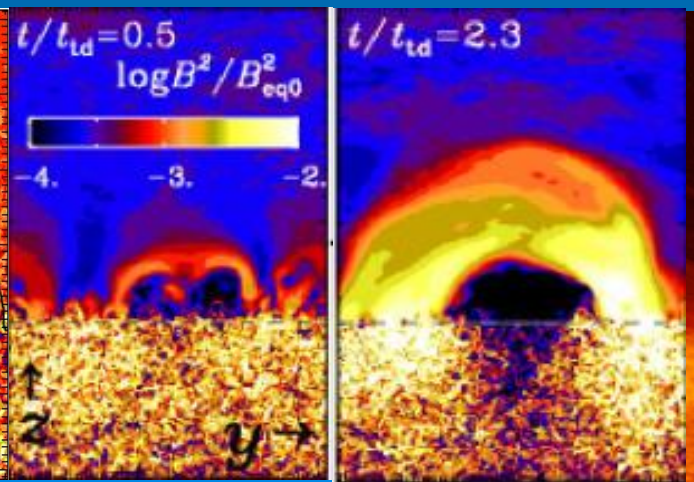

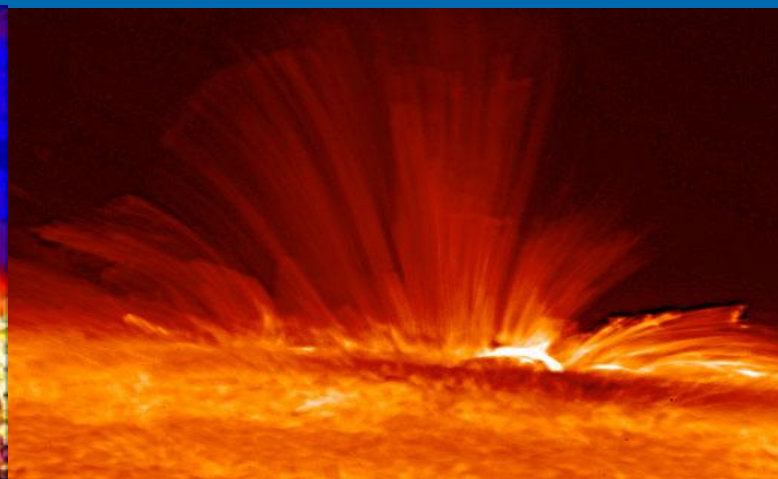

Problems

- What is the mechanism of formation of large-scale magnetic structures in turbulent plasma with large beta?
- Dynamo mechanism can generate only weak nearly uniform large-scale magnetic field.
- How is it possible to create strongly inhomogeneous magnetic structures from originally uniform magnetic field?

Active regions and Sunspots

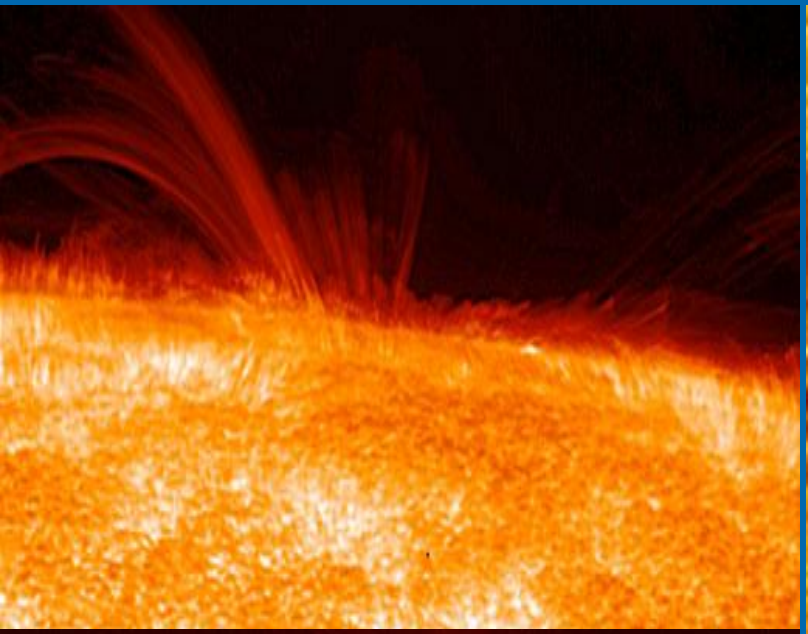

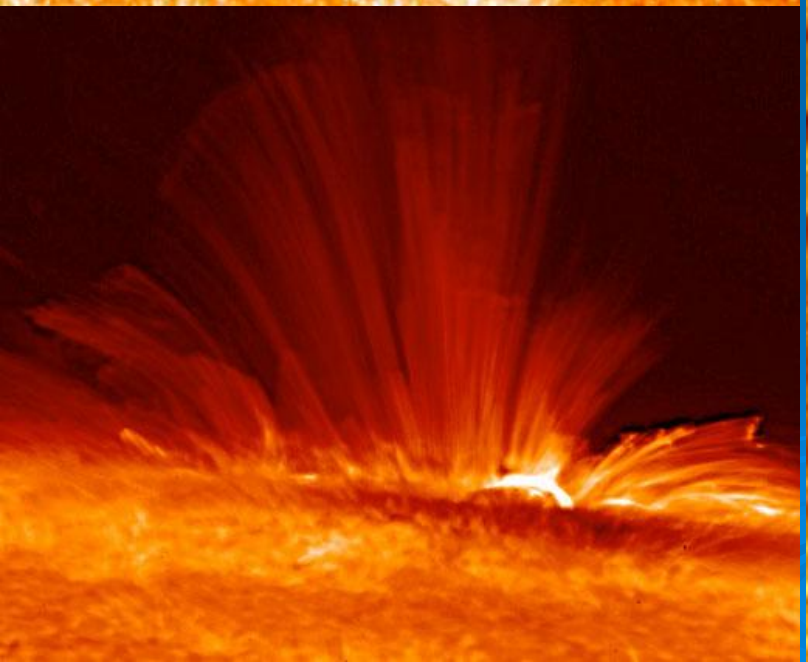

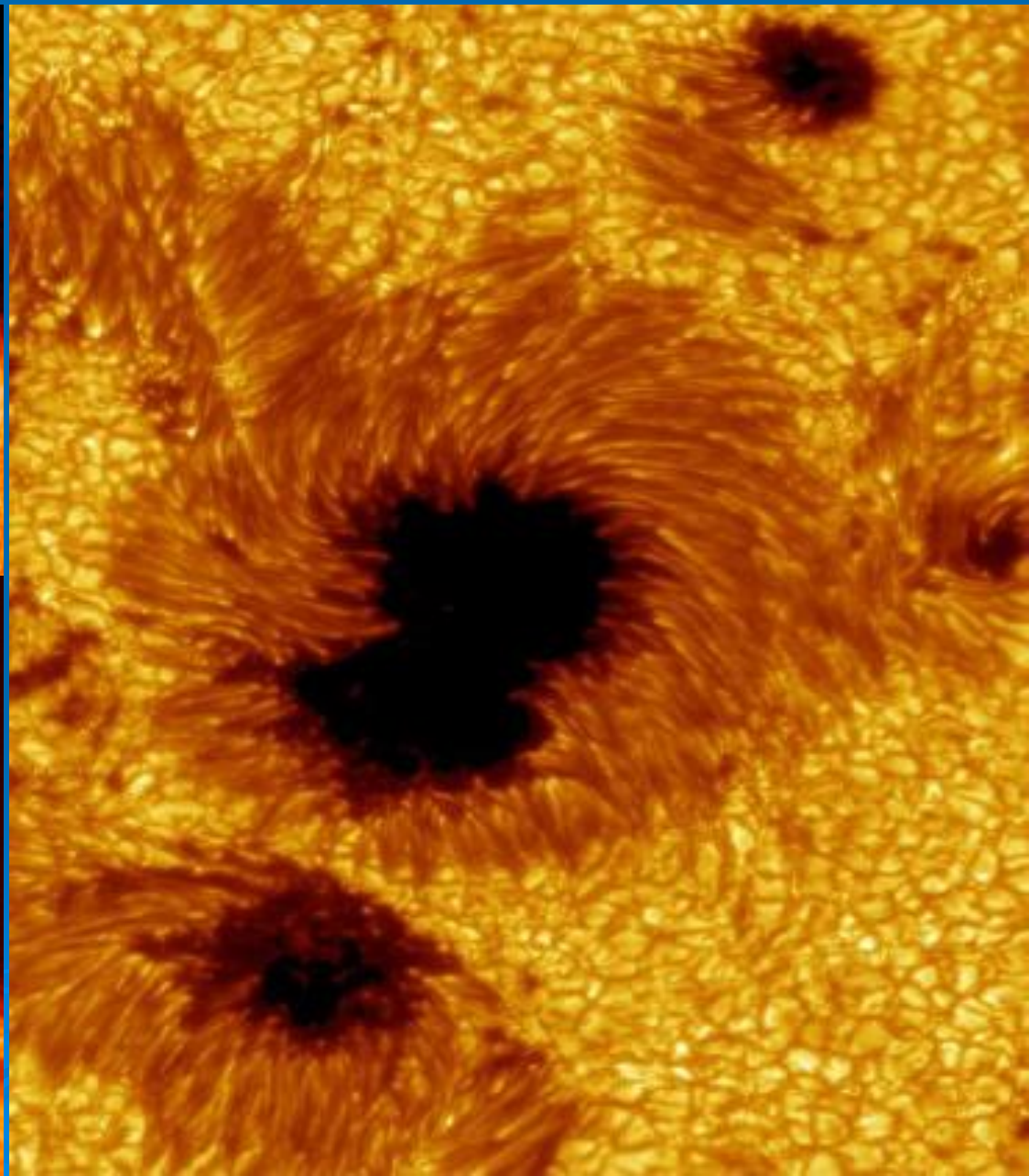

Active regions

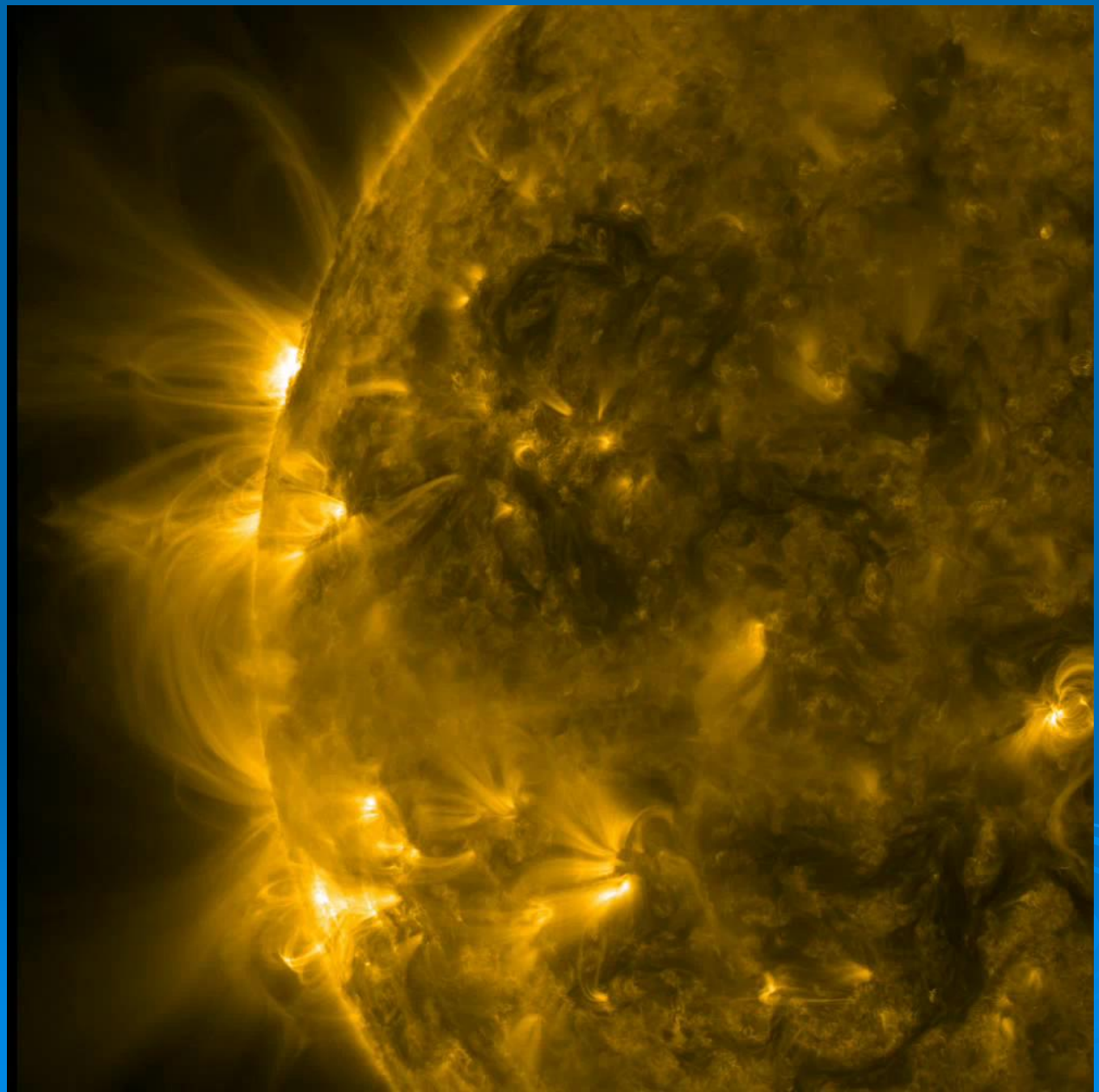

Theories of Magnetic Structure Formation

- 1. Interchange Instability (Magnetic Buoyancy Instability)
- 2. Negative Effective Magnetic Pressure Instability (NEMPI)

Magnetic Buoyancy Instability (Interchange Instability)

Let us estimate the growth rate of this instability. Neglecting dissipative processes for simplicity's sake, we shall retain only the Archimedes force in the momentum equation of the magnetic flux tube

$$\frac{d^2\zeta}{dt^2} = -\left(\frac{C_A}{C_s}\right)^2 \frac{gQ_p(L_B - L_\rho)}{L_B L_\rho}\zeta \ ,$$

where $C_A = \bar{B}_a/\sqrt{\mu\rho_a}$ is the Alfven velocity. The growth rate of this instability is given by

$$\gamma \simeq \frac{C_A}{L_\rho}\left[Q_p\left(\frac{L_\rho}{L_B} - 1\right)\right]^{1/2} \ .$$

Here $L_\rho \simeq C_s^2/g$.

For a weak turbulence ($Q_p \approx 1$), the small-scale turbulence will not affect large-scale processes. The criterion for instability due to buoyancy is $L_B < L_\rho$, and the instability is excited if the scale for change in the initial magnetic field is less than the density scale-height (Parker 1966).

Different Effects of Turbulence

- Turbulent viscosity
- Turbulent diffusion
- Turbulent magnetic diffusion
- Alpha effect
- Turbulent diamagnetic or paramagnetic velocity
- Lambda effect – generation of differential rotation (generation of zonal flows)

Lorentz Force and Momentum Equation

$$\mathbf{J}\times\mathbf{B} = (\boldsymbol{\nabla}\times\mathbf{B})\times\mathbf{B} = -\boldsymbol{\nabla}\frac{\mathbf{B}^2}{2} + (\mathbf{B}\cdot\boldsymbol{\nabla})\mathbf{B} = -\nabla_j\left[\frac{1}{2}B^2\delta_{ij} - B_iB_j\right]$$

$$\frac{\partial}{\partial t}\rho\,\mathbf{U}_i = -\nabla_j\,\Pi_{ij}$$

where

$$\Pi_{ij} = \rho\,U_iU_j + \delta_{ij}\,(p + \frac{1}{2}\mathbf{B}^2) - B_iB_j - \sigma^{\nu}_{ij}(\mathbf{U}) + \ldots$$

Averaged equation: $\mathbf{U} = \bar{\mathbf{U}} + \mathbf{u}\,, \qquad \mathbf{B} = \bar{\mathbf{B}} + \mathbf{b}$

$$\frac{\partial}{\partial t}\bar{\rho}\,\bar{\mathbf{U}}_i = -\nabla_j\,\bar{\Pi}_{ij}$$

where

$$\bar{\Pi}_{ij} = \bar{\rho}\,\bar{U}_i\bar{U}_j + \delta_{ij}\,(\bar{p} + \frac{1}{2}\bar{\mathbf{B}}^2) - \bar{B}_i\bar{B}_j - \bar{\sigma}^{\nu}_{ij}(\bar{\mathbf{U}}) + \frac{1}{2}\langle\mathbf{b}^2\rangle\,\delta_{ij} - \langle b_ib_j\rangle + \bar{\rho}\langle u_iu_j\rangle + \ldots$$

3. Negative Effective Magnetic Pressure Instability (NEMPI)
(sum of turbulent and non-turbulent contributions)

$$\mathbf{J}\times\mathbf{B} = (\boldsymbol{\nabla}\times\mathbf{B})\times\mathbf{B} = -\boldsymbol{\nabla}\frac{\mathbf{B}^2}{2} + (\mathbf{B}\cdot\boldsymbol{\nabla})\mathbf{B} = -\nabla_j\left[\frac{1}{2}B^2\delta_{ij} - B_iB_j\right]$$

A. Brandenburg, K. Kemel, N. Kleeorin, I. Rogachevskii, Astrophys. J. 749, 179 (2012)

$$\mathcal{P}_{\rm eff}(\beta) = \tfrac{1}{2}[1 - q_{\rm p}(\beta)]\,\beta^2 \quad \text{versus} \quad \beta \equiv |\overline{\boldsymbol{B}}|/B_{\rm eq}$$

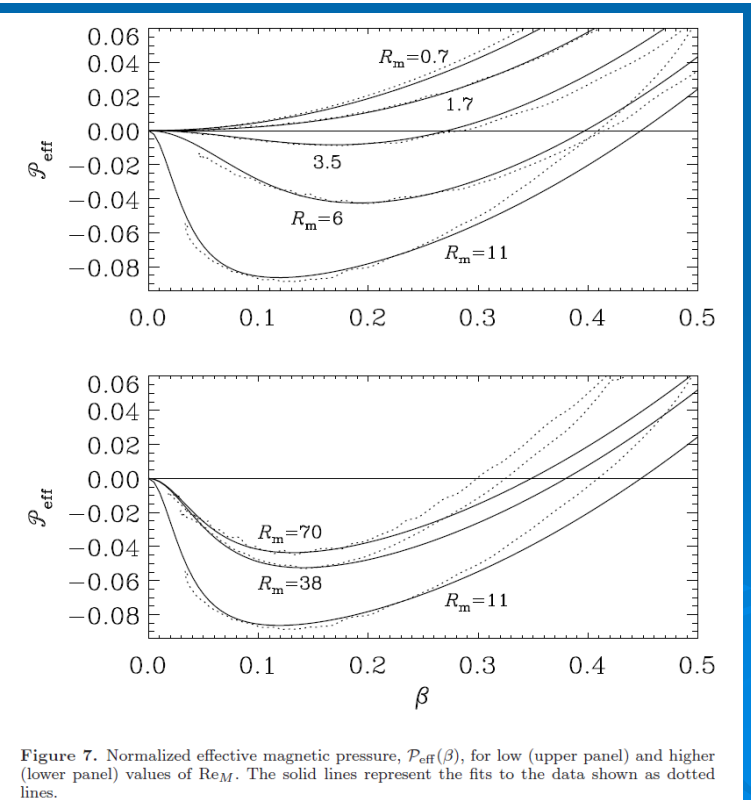

Figure 7. Normalized effective magnetic pressure, $\mathcal{P}_{\rm eff}(\beta)$, for low (upper panel) and higher (lower panel) values of Re_M. The solid lines represent the fits to the data shown as dotted lines.

$$\mathcal{P}_{\rm eff} = \frac{1}{2}(1 - q_p)\frac{\bar{\mathrm{B}}^2}{\mathrm{B}_{\rm eq}^2}$$

Effective magnetic pressure for Rm < 1 is positive, and for Rm > 1, it can be negative.

Quasi-linear theory works only for

$$\mathrm{Rm} \ll 1$$

Equation of State for Isotropic Turbulence

N. Kleeorin, I. Rogachevskii and A. Ruzmaikin, *Sov. Astron. Lett. 15, 274-277 (1989); Sov. Phys. JETP 70, 878-883 (1990)*

N. Kleeorin and I. Rogachevskii, *Phys. Rev. E 50, 2716-2730 (1994)*

I. Rogachevskii and N. Kleeorin, *Phys. Rev. E 76, 056307 (2007)*

The total turbulent pressure is reduced when magnetic fluctuations are generated

The equation of state for an isotropic turbulence

$$p_T = \frac{1}{3} W_m + \frac{2}{3} W_k \ ,$$

where p_T is the total (hydrodynamic plus magnetic) turbulent pressure,

$W_m = \langle \mathbf{b}^2 \rangle / 2\mu$ is the energy density of the magnetic fluctuations,

$W_k = \rho_0 \langle \mathbf{u}^2 \rangle / 2$ is the kinetic energy density.

Strong reduction of Turbulent Pressure

Combining the equations:

$$p_T = \frac{1}{3}W_m + \frac{2}{3}W_k = \frac{2}{3}(W_k + W_m) - \frac{1}{3}\mathrm{W_m}\,, \qquad \mathrm{W_k + W_m = const}\,,$$

we can express the change of turbulent pressure δp_T in terms of the change of the magnetic energy density δW_m

$$\delta \mathrm{p_T} = -\frac{1}{3}\delta \mathrm{W_m}$$

Therefore, the turbulent pressure is reduced when magnetic fluctuations are generated (i.e., $\delta \mathrm{W_m} > 0$).

Total Turbulent Energy

The total energy density W_T of the homogeneous turbulence with a nonzero uniform mean magnetic field is conserved

$$\mathrm{W_k + W_m = const.}$$

The uniform large-scale magnetic field performs no work on the turbulence. It can only redistribute the energy between hydrodynamic fluctuations and magnetic fluctuations.

The total energy density $\mathrm{W_T = W_k + W_m}$ of the homogeneous turbulence with a mean magnetic field $\bar{\mathrm{B}}$

$$\frac{\partial W_T}{\partial t} = I_T - \frac{W_T}{\tau_0} + \eta_T \frac{(\boldsymbol{\nabla} \times \bar{\mathrm{B}})^2}{\mu}$$

$I_T =$ is the energy source of turbulence,

W_T/τ_0 determines the dissipation of the turbulent energy.

Equation of State for Anisotropic Turbulence

The equation of state for an anisotropic turbulence

$$p_T = \frac{1}{3(1+\sigma/2)} W_m + \frac{2}{3}\left(\frac{1+3\sigma/4}{1+\sigma/2}\right) W_k \,,$$

where $0 \leq \sigma < \infty$ is the degree of anisotropy of turbulence. For a two-dimensional turbulence: $\sigma \to \infty$ and the equation of state reads:

$$p_T = \frac{2}{3\sigma} W_m + W_k = (W_k + W_m) - \mathbf{W_m} \,,$$

Thus, the change of turbulent pressure δp_T for the two-dimensional turbulence is

$$\delta \mathbf{p_T} = -\delta \mathbf{W_m}$$

Effective Magnetic Pressure

The total pressure is

$$p_{tot} = p_k + p_T + P_B(\bar{B}) \ ,$$

where p_k is the fluid pressure and $P_B(\bar{B}) = \frac{\bar{\mathrm{B}}^2}{2\mu}$ is the magnetic pressure of the mean field.

Now we examine the part in p_{tot} that depends on the mean (large-scale) magnetic field $\bar{\mathrm{B}}$:

$$\mathrm{P_m(\bar{B})} = P_B(\bar{B}) - \mathrm{q_p(\bar{B})}\frac{\bar{\mathrm{B}}^2}{2\mu} = (1 - \mathrm{q_p(\bar{B})})\frac{\bar{\mathrm{B}}^2}{2\mu} \equiv Q_p(\bar{B})\frac{\bar{\mathrm{B}}^2}{2\mu} \ ,$$

$$p_{\mathrm{tot}} = p + \mathrm{P_m(\bar{B})} = p + \mathrm{Q_p(\bar{B})}\frac{\bar{\mathrm{B}}^2}{2\mu} \ ,$$

where $p = p_k + p_T^{(0)}$. The pressure $P_m(\bar{B})$ is the combined mean magnetic pressure.

DNS: The Result is Robust

$$\mathcal{P}_{\rm eff} = \frac{1}{2}(1 - q_p)\frac{\bar{\rm B}^2}{\rm B_{eq}^2}$$

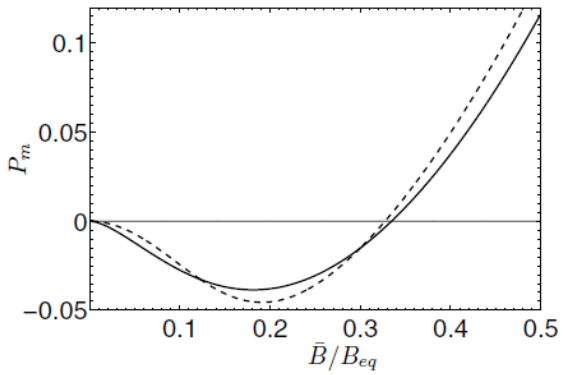

Fig. 3 The effective mean magnetic pressure $P_m(\overline{B}) = (1 - q_{\rm p})\overline{B}^2/\overline{B}_{\rm p}^2$ determined by Rogachevskii & Kleeorin (2007) – solid line, and by the model described by Eq. (26) – dashed line ($\overline{B}_{\rm p} = 0.21\, c_{\rm s0}\rho_0^{1/2}$ and $q_{\rm p0} = 4$).

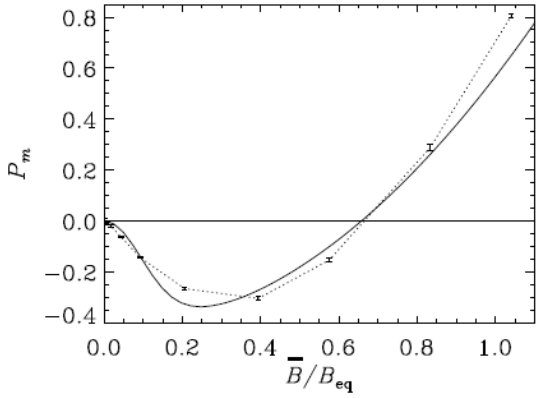

Fig. 4 Same as Fig. 3, but from simulation (dotted line). The solid line shows a fit [Eq. (26)] with $\overline{B}_{\rm p} = 0.022\, c_{\rm s0}\rho_0^{1/2}$ (corresponding to $\overline{B}_{\rm p}/B_{\rm eq} = 0.18$) and $q_{\rm p0} = 21$.

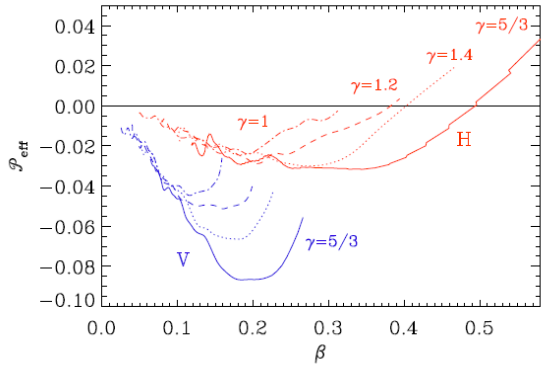

Fig. 7. Effective magnetic pressure obtained from DNS in a polytropic layer with different γ for horizontal (H, red curves) and vertical (V, blue curves) mean magnetic fields.

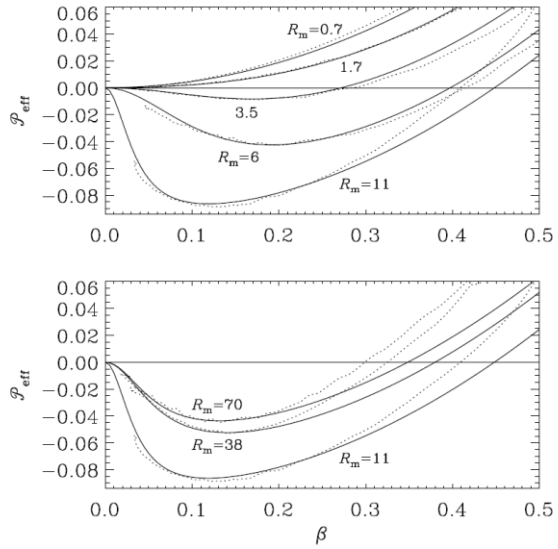

Figure 7. Normalized effective magnetic pressure, $\mathcal{P}_{\rm eff}(\beta)$, for low (upper panel) and higher (lower panel) values of Re_M. The solid lines represent the fits to the data shown as dotted lines.

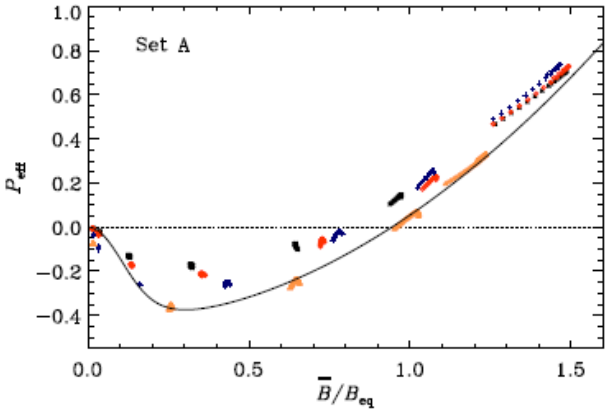

Figure 2. Effective magnetic pressure as a function of the mean magnetic field from weakly stratified Runs A1–A29 with an imposed horizontal field $\boldsymbol{B}_0 = B_0\hat{\boldsymbol{x}}$. The black stars, red diamonds, blue crosses, and yellow triangles denote simulations with Rm $\approx$ 10, 20, 50, and 70, respectively. We omit points near the boundaries at $z/d < 0.35$ and $z/d > 0.65$. The dashed and dotted lines correspond to approximate fits determined by Eq. (30), with $q_{p0} = 35$ and $B_p = 0.2B_{\rm eq}$, respectively.

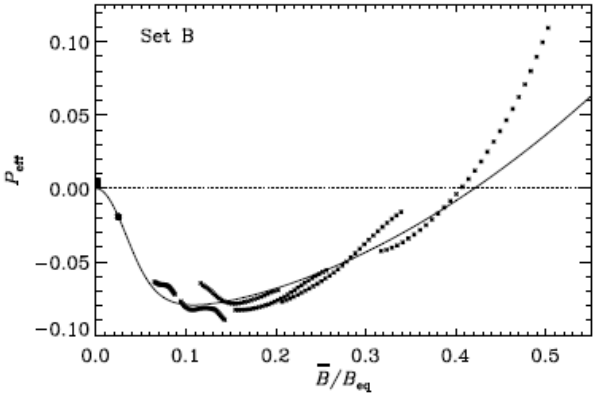

Figure 3. Same as Figure 2 but for Runs B1–B8 for Rm = 40–50. The solid line corresponds to a fit with $q_{p0} = 70$ and $B_p = 0.063B_{\rm eq}$

Methods and Approximations

- **Quasi-Linear Approach** or Second-Order Correlation Approximation (SOCA) or First-Order Smoothing Approximation (FOSA); **Rm << 1 , Re << 1**

N. Kleeorin, I. Rogachevskii and A. Ruzmaikin, *Sov. Phys. JETP 70, 878-883 (1990)*
A. Brandenburg, K. Kemel, N. Kleeorin, I. Rogachevskii, Astrophys. J. 749, 179 (2012)

- **Tau-approaches** (spectral tau-approximation) – **third-order or high-order closure; Re >> 1 and Rm >> 1**

N. Kleeorin, I. Rogachevskii and A. Ruzmaikin, *Sov. Phys. JETP 70, 878-883 (1990)*
I. Rogachevskii and N. Kleeorin, *Phys. Rev. E 76, 056307 (2007)*

- **Renormalization Procedure** (renormalization of turbulent transport coefficients) - **Re >> 1 and Rm >> 1, there is no separation of scales.**

N. Kleeorin and I. Rogachevskii, *Phys. Rev. E 50, 2716-2730 (1994)*

NEMPI in DNS: 3D Forced Turbulence (Vertical Imposed Weak Magnetic Field)

All simulations are performed with the PENCIL CODE, that uses sixth-order explicit finite differences in space and a third-order accurate time stepping method.

$$\rho\frac{\mathrm{D}\boldsymbol{U}}{\mathrm{D}t} = -c_{\mathrm{s}}^2\boldsymbol{\nabla}\rho + \boldsymbol{J}\times\boldsymbol{B} + \rho(\boldsymbol{f}+\boldsymbol{g}) + \boldsymbol{\nabla}\cdot(2\nu\rho\mathbf{S}),$$

$$\frac{\partial \boldsymbol{A}}{\partial t} = \boldsymbol{U}\times\boldsymbol{B} + \eta\nabla^2\boldsymbol{A},$$

$$\frac{\partial \rho}{\partial t} = -\boldsymbol{\nabla}\cdot\rho\boldsymbol{U},$$

$$\boldsymbol{B} = \boldsymbol{B}_0 + \boldsymbol{\nabla}\times\boldsymbol{A}$$

$512^3; 1024^3$

$$\mathrm{Pm} = \frac{\nu}{\eta} = \frac{1}{2}$$

$$k_f = 30\,k_1;$$

$$\frac{\rho_{bot}}{\rho_{top}} = 535;$$

BOUNDARY CONDITIONS at the top and bottom:

$$U_z = 0, \quad \nabla_z U_x = \nabla_z U_y = 0$$

$$B_x = B_y = 0,$$

BOUNDARY CONDITIONS:

1). The horizontal boundaries are periodic.

2). For the velocity we apply impenetrable, stress-free conditions.

3). For the magnetic field we use vertical field boundary conditions.

Formation of Magnetic Spots in DNS

(Vertical Imposed Weak Magnetic Field)

PENCIL CODE

$256^3; 512^3; 1024^3$

$k_f = 30\, k_1;$

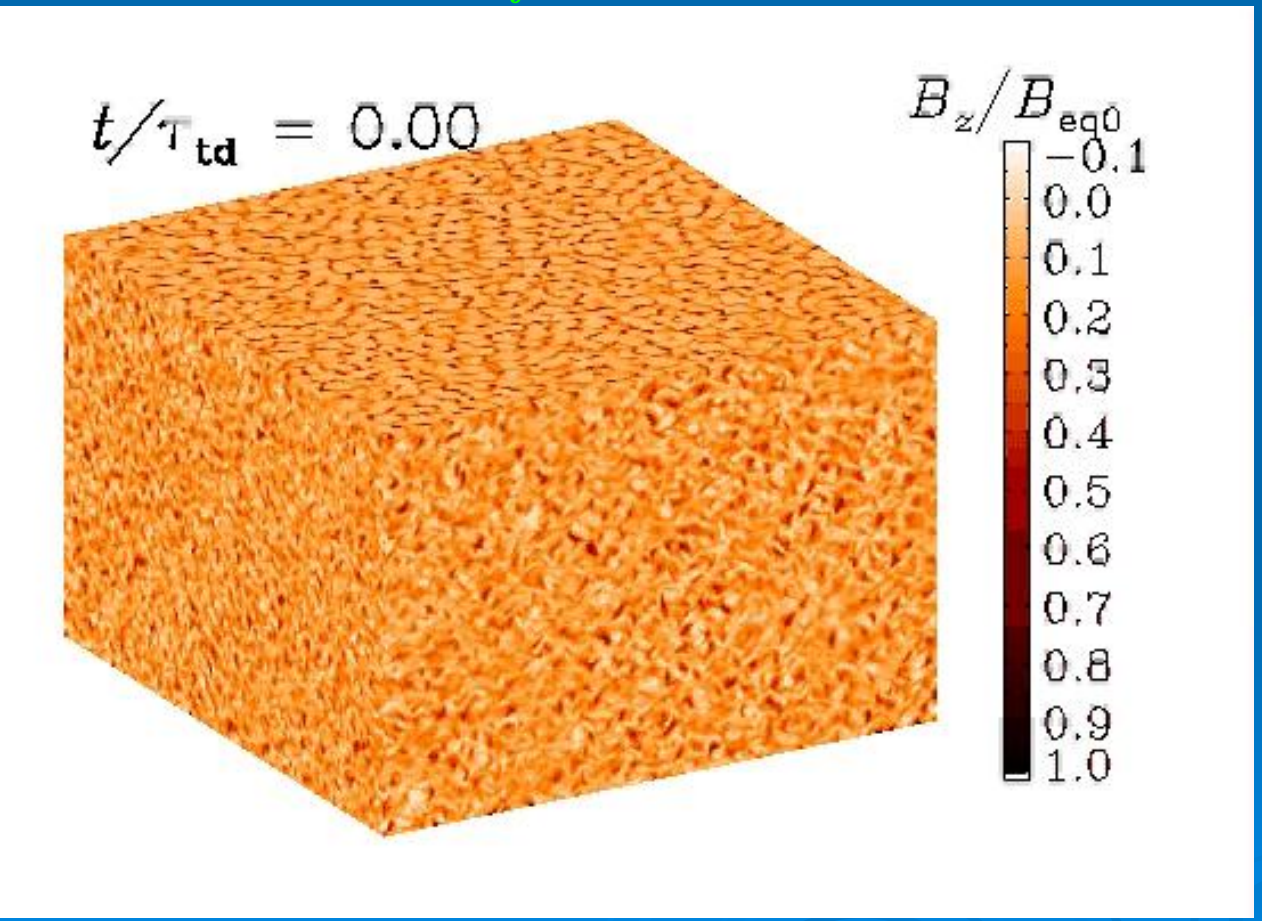

$$\mathrm{Rm} = \frac{u_{rms}}{\eta\, k_f} = 18; 40; 95$$

$$\mathrm{Pm} = \frac{\nu}{\eta} = \frac{1}{2}$$

$$\frac{\rho_{bot}}{\rho_{top}} = 535;$$

BOUNDARY CONDITIONS at the top and bottom:

1. stress-free conditions

$$\nabla_z U_x = \nabla_z U_y = 0$$
$$U_z = 0,$$

2. vertical field

$$B_x = B_y = 0,$$

A. Brandenburg, N. Kleeorin and I. Rogachevskii, Astrophys. J. Lett., 776, L23 (2013)

Linear Phase of NEMPI

A. Brandenburg, N. Kleeorin and I. Rogachevskii, Astrophys. J. Lett., 776, L23 (2013)

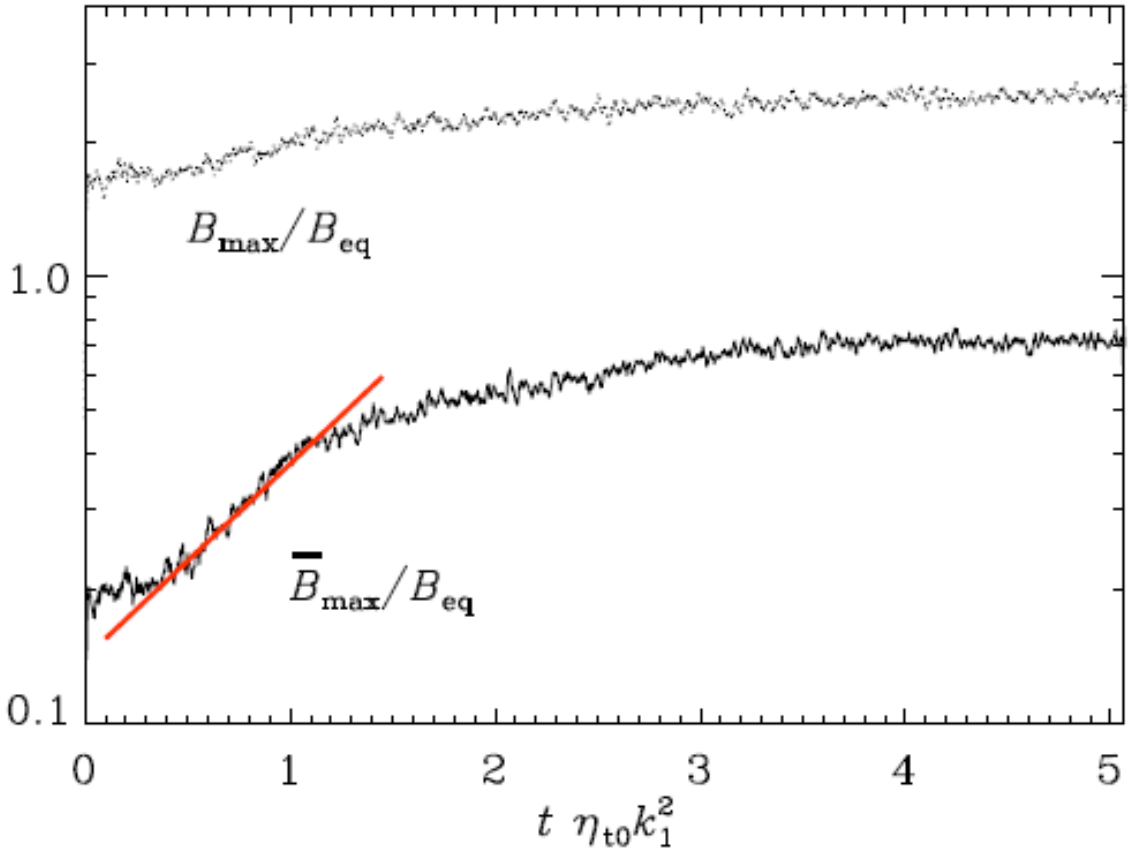

FIG. 2.— Growth of $\overline{B}_{\rm max}/B_{\rm eq}$ (solid line) and $B_{\rm max}/B_{\rm eq}$ (dotted line) at the top of the domain. The straight red line gives a fit to $\overline{B}_{\rm max}/B_{\rm eq}$ with a slope of unity corresponding to the growth rate $(\eta_{\rm t0}k_1^2)^{-1}$.

$$\lambda = \frac{v_{\rm A}}{H_\rho}\left(-2\frac{{\rm d}\mathcal{P}_{\rm eff}}{{\rm d}\beta^2}\right)^{1/2}\frac{k_x}{k}.$$

$$\mathcal{P}_{\rm eff} = \frac{1}{2}(1-q_p)\frac{\bar{\rm B}^2}{\rm B_{eq}^2}$$

Time-evolution of the Magnetic Spot

A. Brandenburg, N. Kleeorin and I. Rogachevskii, Astrophys. J. Lett., 776, L23 (2013)

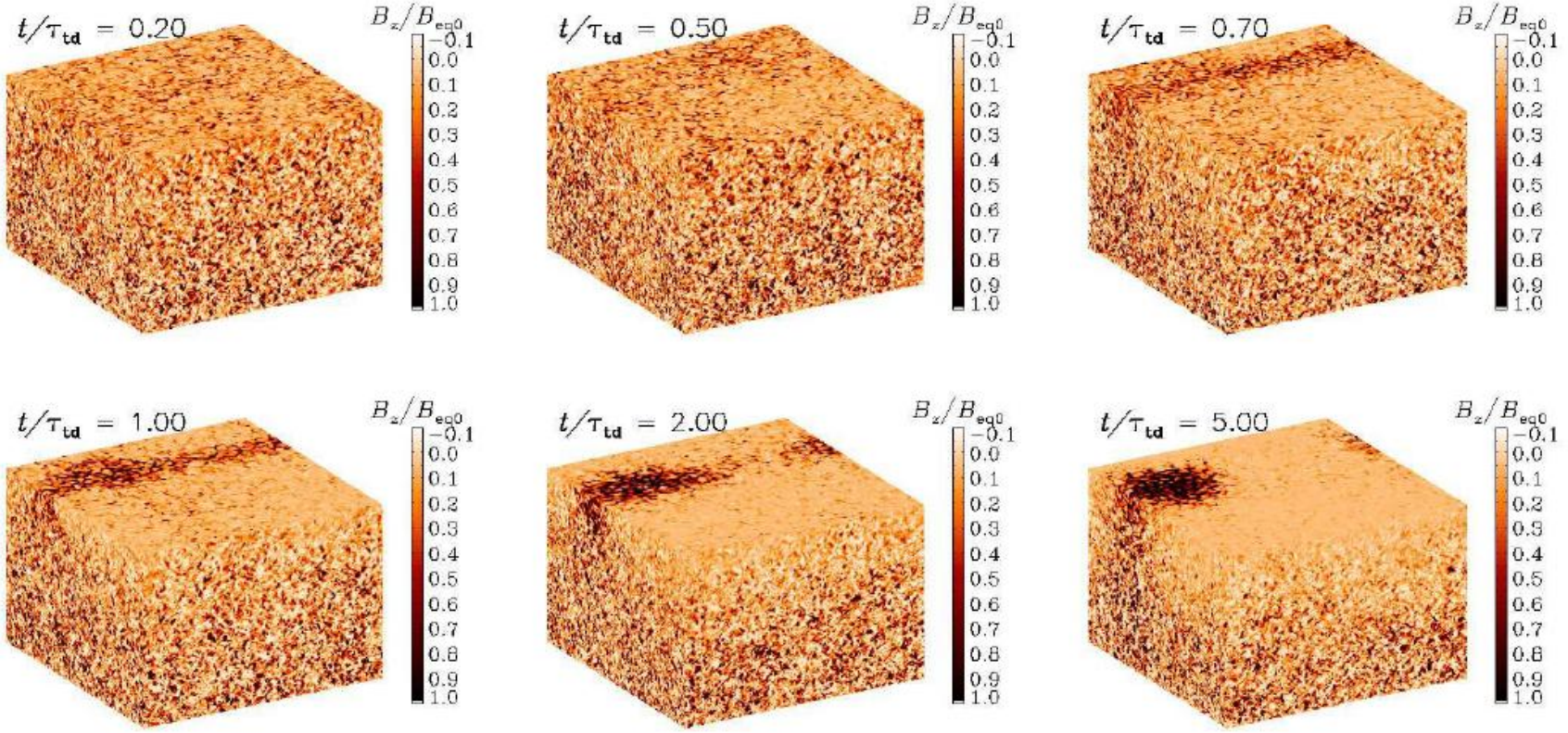

FIG. 1.— Evolution from a statistically uniform initial state toward a single spot for $B_{z0}/B_{eq0} = 0.02$. Here, B_z/B_{eq0} is shown on the periphery of the domain. Dark shades correspond to strong vertical fields. Time is in units of τ_{td}.

Structure of the Magnetic Spot

A. Brandenburg, N. Kleeorin and I. Rogachevskii, Astrophys. J. Lett., 776, L23 (2013)

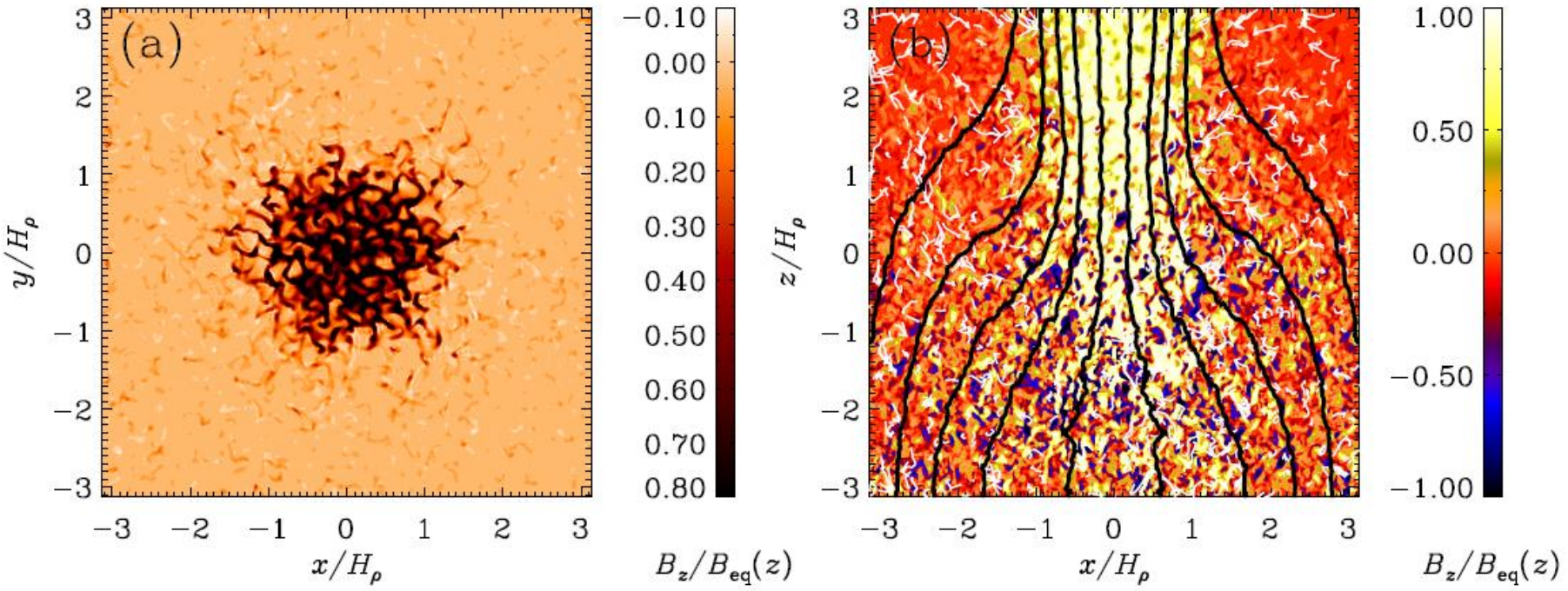

FIG. 3.— Cuts of $B_z/B_{eq}(z)$ in the xy plane at the top boundary ($z/H_\rho = \pi$) and the xz plane through the middle of the spot at $y = 0$. In the xz cut, we also show magnetic field lines and flow vectors obtained by numerically averaging in azimuth around the spot.

$\mathrm{Pr}_M = 0.06 - 1$

Formation and Destruction of Bipolar Magnetic Structures

J. Warnecke, I.R. Losada, A. Brandenburg, N. Kleeorin and I. Rogachevskii,
Astrophys. J. Lett., 777, L37 (2013); Astron. Astrophys., 589, A125 (2016).

Imposed horizontal field.

$k_f = 30\, k_1;$

512 x 512 x 1024; 1024^3

BOUNDARY CONDITIONS at the top and bottom:

$U_z = 0, \quad \nabla_z U_x = \nabla_z U_y = 0$

But

$z = -\pi$:

$B_z = 0, \quad \nabla_z B_x = \nabla_z B_y = 0$

$z = 2\pi$:

$B_x = B_y = 0.$

Re=40, $\mathrm{Pr}_M = 0.06 - 1$

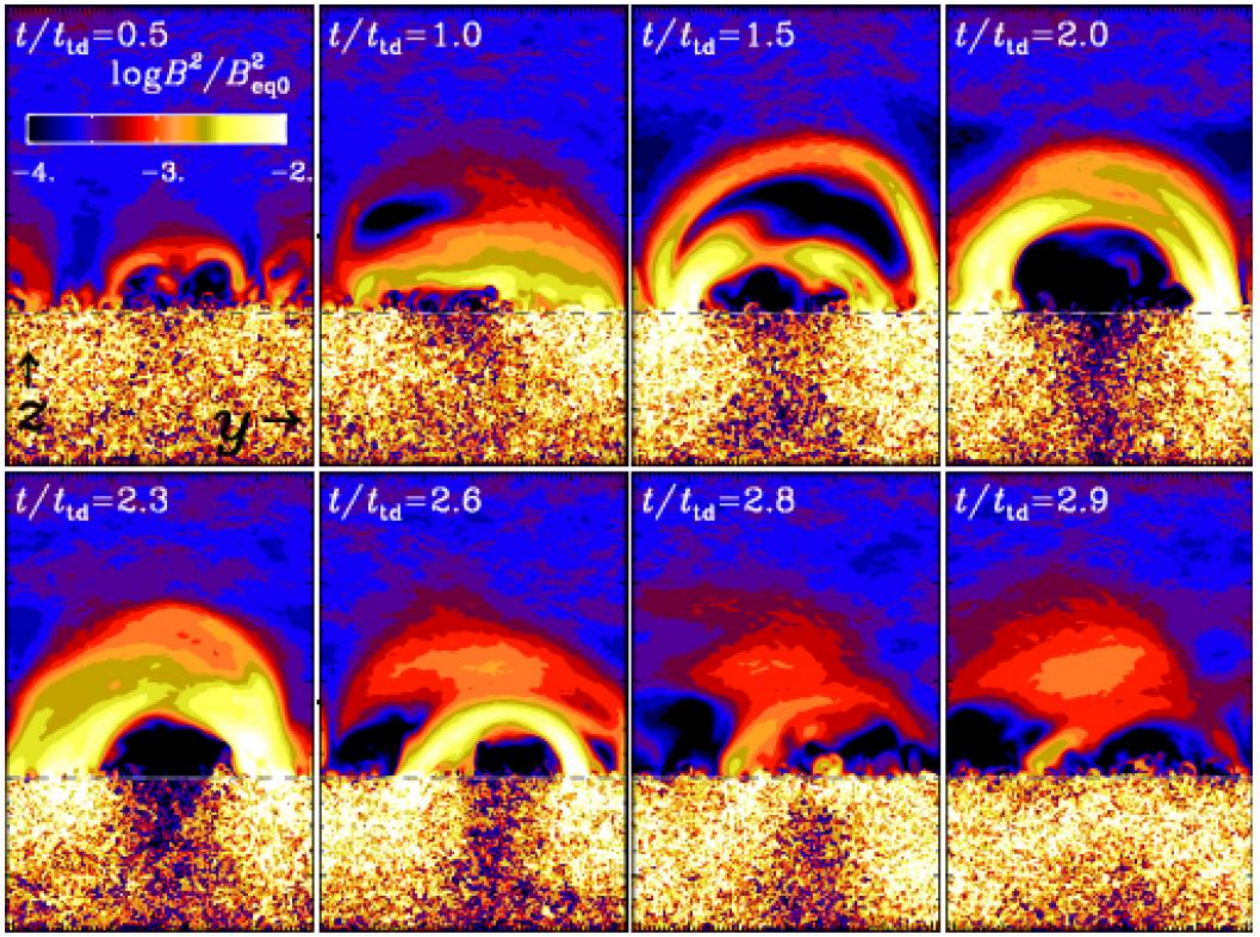

FIG. 5.— Time series of B^2/B^2_{eq0} in a vertical cut through the bipolar region at $x = 0$. Note the y axis is shifted the see the formation of the loop.

Formation and Destruction of Bipolar Magnetic Structures

J. Warnecke, I.R. Losada, A. Brandenburg, N. Kleeorin and I. Rogachevskii,
Astrophys. J. Lett., 777, L37 (2013); Astron. Astrophys., 589, A125 (2016).

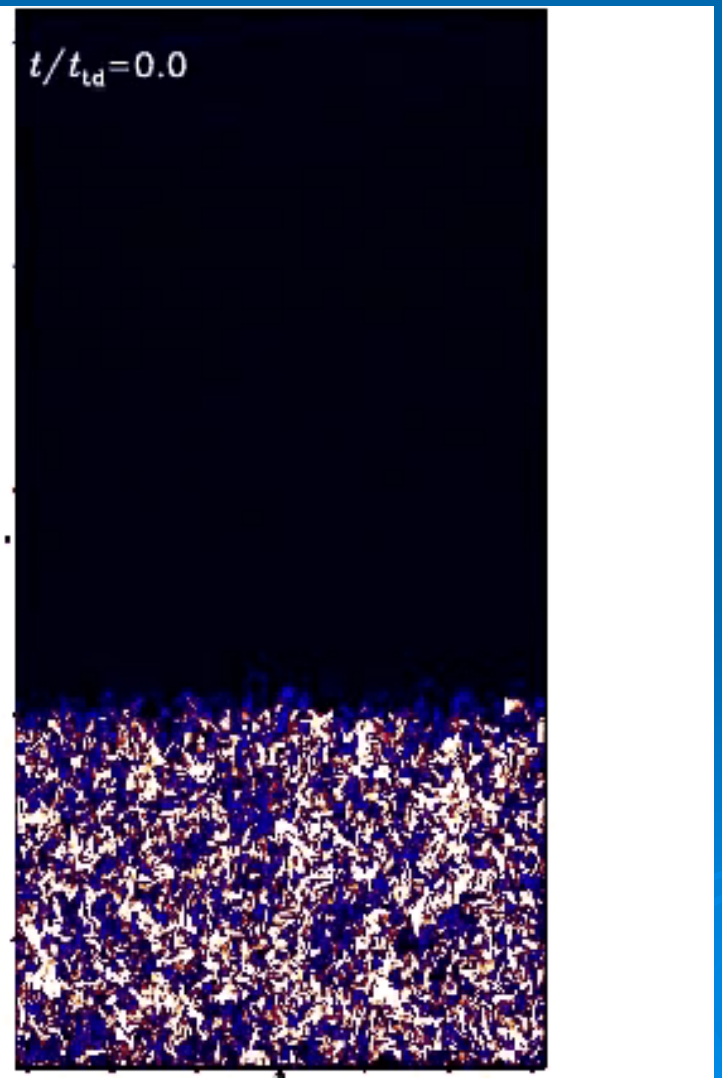

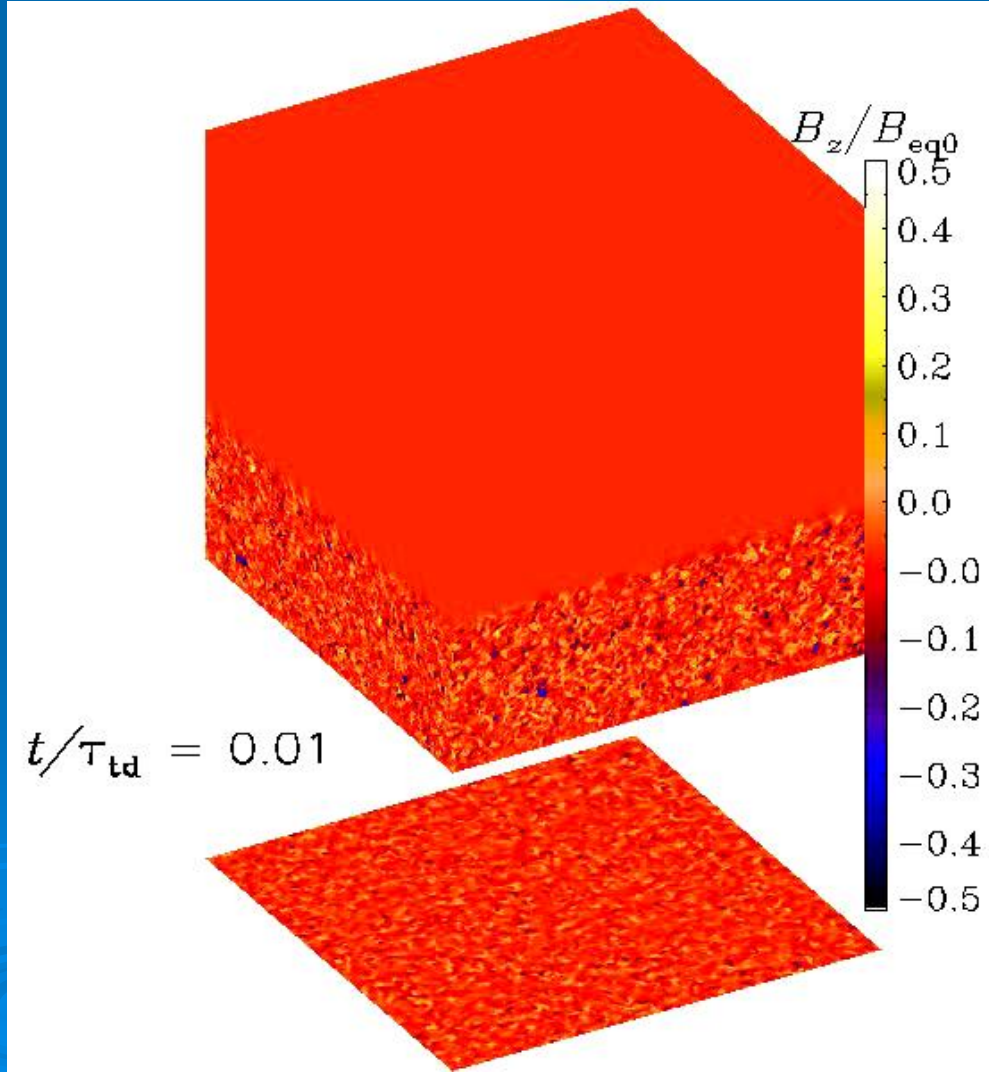

Magnetic Structures

J. Warnecke, I.R. Losada, A. Brandenburg, N. Kleeorin and I. Rogachevskii, Astrophys. J. Lett., 777, L37 (2013), Astron. Astrophys., 589, A125 (2016).

Simulations

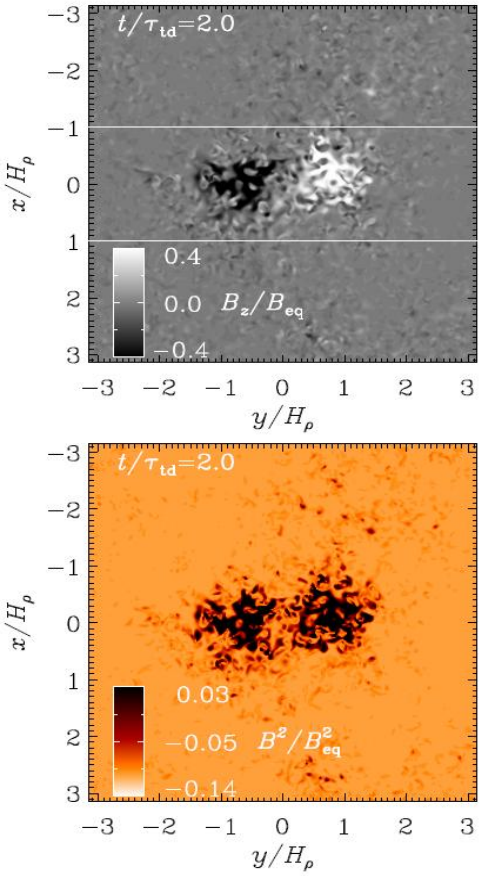

FIG. 1.— *Upper panel:* normalized vertical magnetic field B_z/B_{eq} of the bipolar region at the surface ($z = 0$) of the simulation domain. The white lines delineate the area shown in Figure 3. *Lower panel:* normalized magnetic energy B^2/B_{eq}^2 of the two regions relative to the rest of the surface. Note that we clip both color tables to increase the visualization of the structure. The field strength reaches around $B_z/B_{eq} = 1.4$.

Sunspots

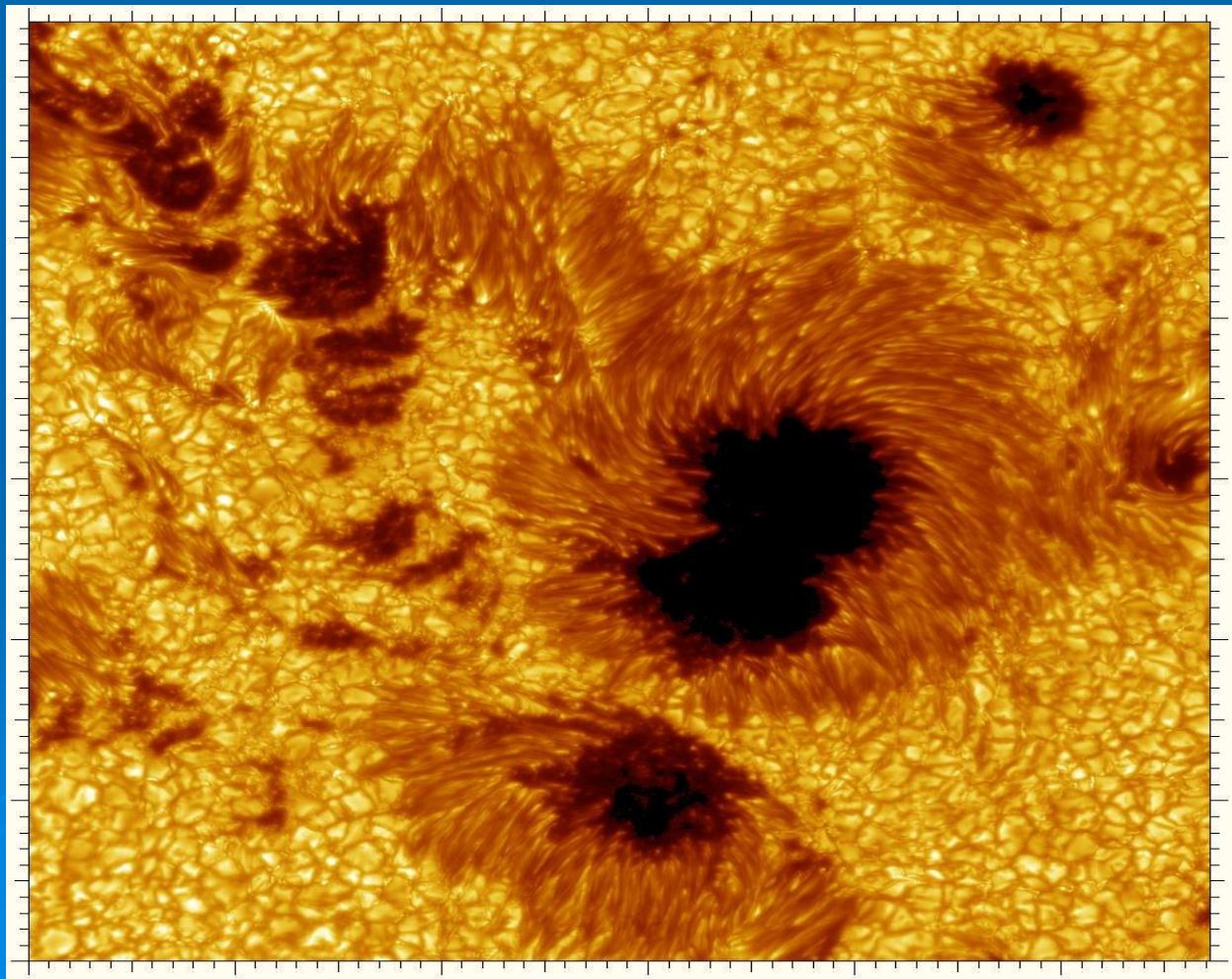

Simulations: DNS and MFS

Vertical Imposed Field in Polytropic Atmosphere

I.R. Losada, A. Brandenburg, N. Kleeorin, I. Rogachevskii,
Astron. Astrophys. 564, A2, (2014);

$$p(z) = \rho^{\gamma} \qquad \gamma = 5/3$$

DNS

MFS

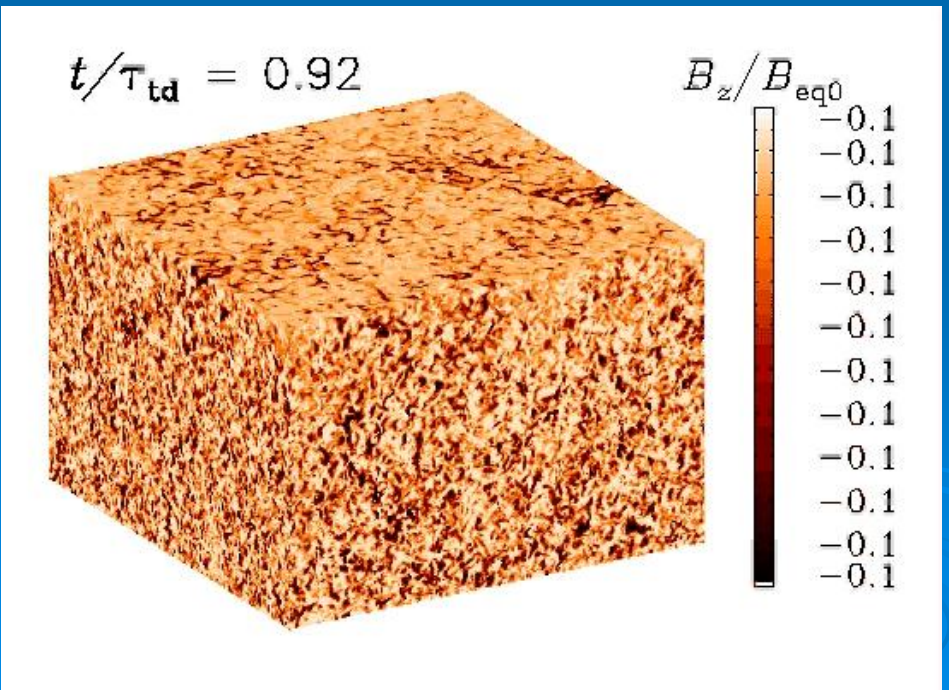

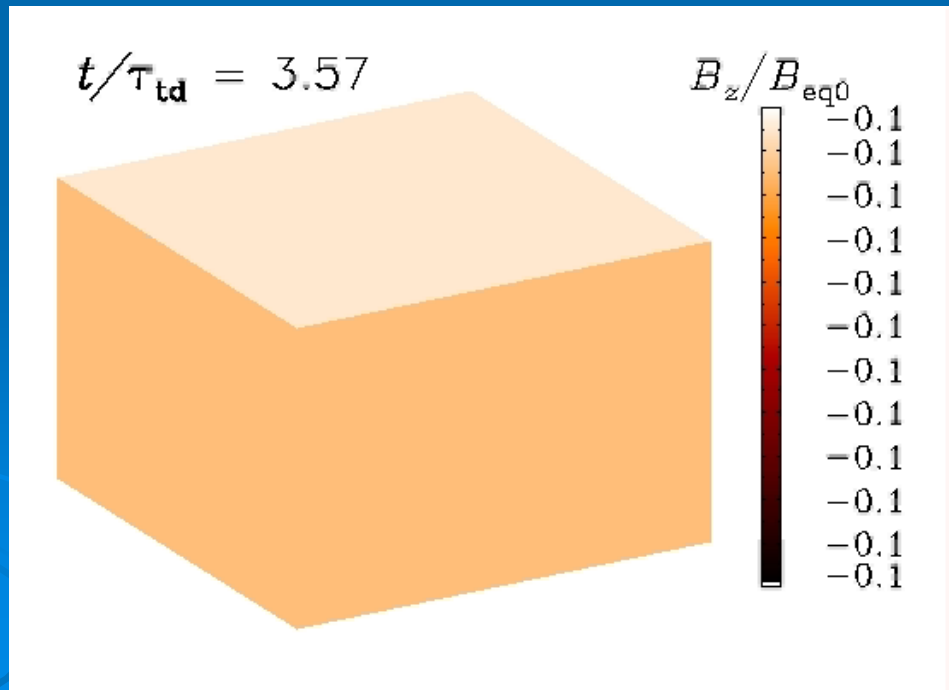

DNS and Mean-Field Simulations

$\gamma = 5/3$

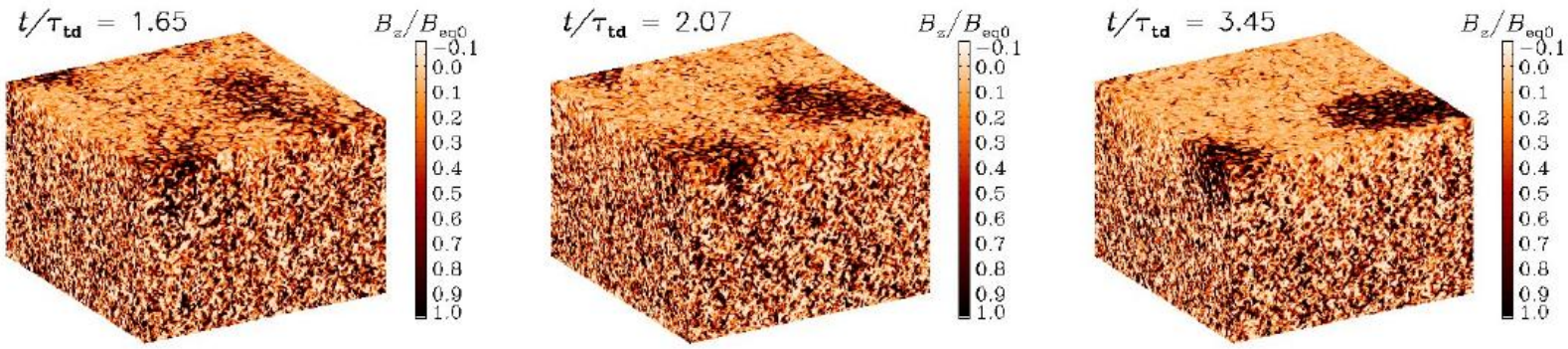

Fig. 5. Snapshots from DNS showing $\overline{B}_z$ on the periphery of the computational domain for $\gamma = 5/3$ and $\beta_0 = 0.05$ at different times for the case of a vertical field using the vertical field boundary condition.

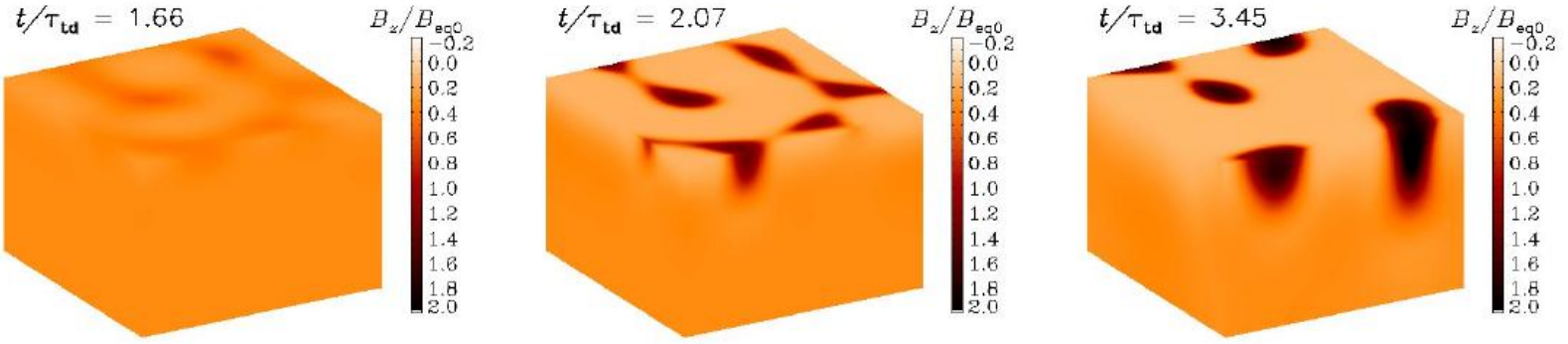

Fig. 17. Similar to Fig. 16 of MFS, but for Model II at times similar to those in the DNS of Fig. 5. Note that there are now more structures than in the earlier MFS of Fig. 16, and that they develop more rapidly.

ILES-Formation of Magnetic Flux Tubes (Vertical Imposed Weak Magnetic Field)

Brandenburg A., Gressel O., Jabbari S., Kleeorin N., and Rogachevskii I., Astron. Astrophys. 562, A53 (2014).

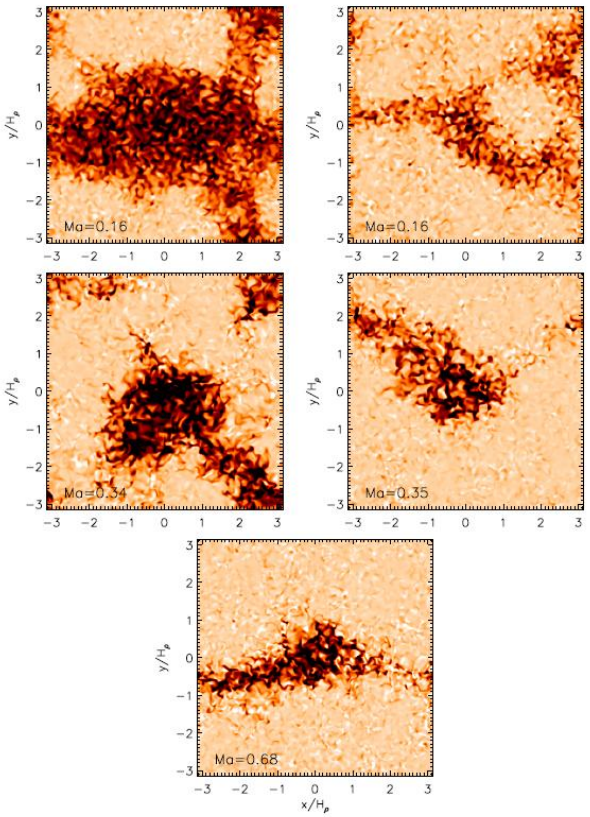

Fig. 22. Surface appearance of the vertical magnetic field, $B_z^{\max}$, in the ILES simulations with different Mach numbers (*top to bottom*). The color coding shows $B_z^{\max}/B_{\rm eq}$ in the range of −0.1 (white) to +1.0 (black). Root-mean-square Mach numbers are given by the labels. For the *upper two rows* with lower Mach number, the *left column* is for fixed initial mean field, whereas in the *right column* the initial field is adjusted between the runs, such that the field strength remains constant relative to the kinetic energy in the background turbulence.

Boundary conditions are

1. Periodic in the horizontal directions,
2. Stress free on the upper and lower boundaries.
3. The magnetic field is assumed to be vertical.

The results from ILES are in good agreement with the DNS. This demonstrates that the mechanism causing magnetic flux concentrations by NEMPI is robust and not sensitive to details of the magnetic Reynolds numbers.

As the Mach number is increased, the magnetic structures become smaller.

$$\hat{\overline{B}} = \overline{B}/B_{\rm eq}$$

Table 6. Summary of DNS and ILES at varying values of Ma, all for $\hat{q} = 3$, $\hat{k}_{\rm f} = 30$.

Run	$\tilde{B}_0$	Re_M	Ma	$\hat{\lambda}$	$\hat{B}_z$	$\hat{\overline{B}}_z$
D01	0.01	24	0.15	0.28	3.06	0.78
D02	0.02	24	0.14	0.46	4.47	1.31
D10	0.10	8	0.50	0.25	4.91	1.61
I03	0.10	–	0.16	>1	2.86	1.14
I10	0.10	–	0.34	>1	2.70	1.00
I30	0.10	–	0.68	>1	2.41	1.02

Notes. For ILES, no accurate values of $\hat{\lambda}$ are available. In the DNS, the resolution is 256^2 for Runs D01 and D02, and 512^2 for Run D10, while for Runs I03–I30 it is $256^2 \times 128$.

ILES-Formation of Magnetic Flux Tubes (Vertical Imposed Weak Magnetic Field)

ILES are DNS without explicit physical dissipation coefficients (the dissipation scales are not resolved, but no turbulence parameterization model is used to represent the unresolved scales). The finite-volume code Nirvana is used.

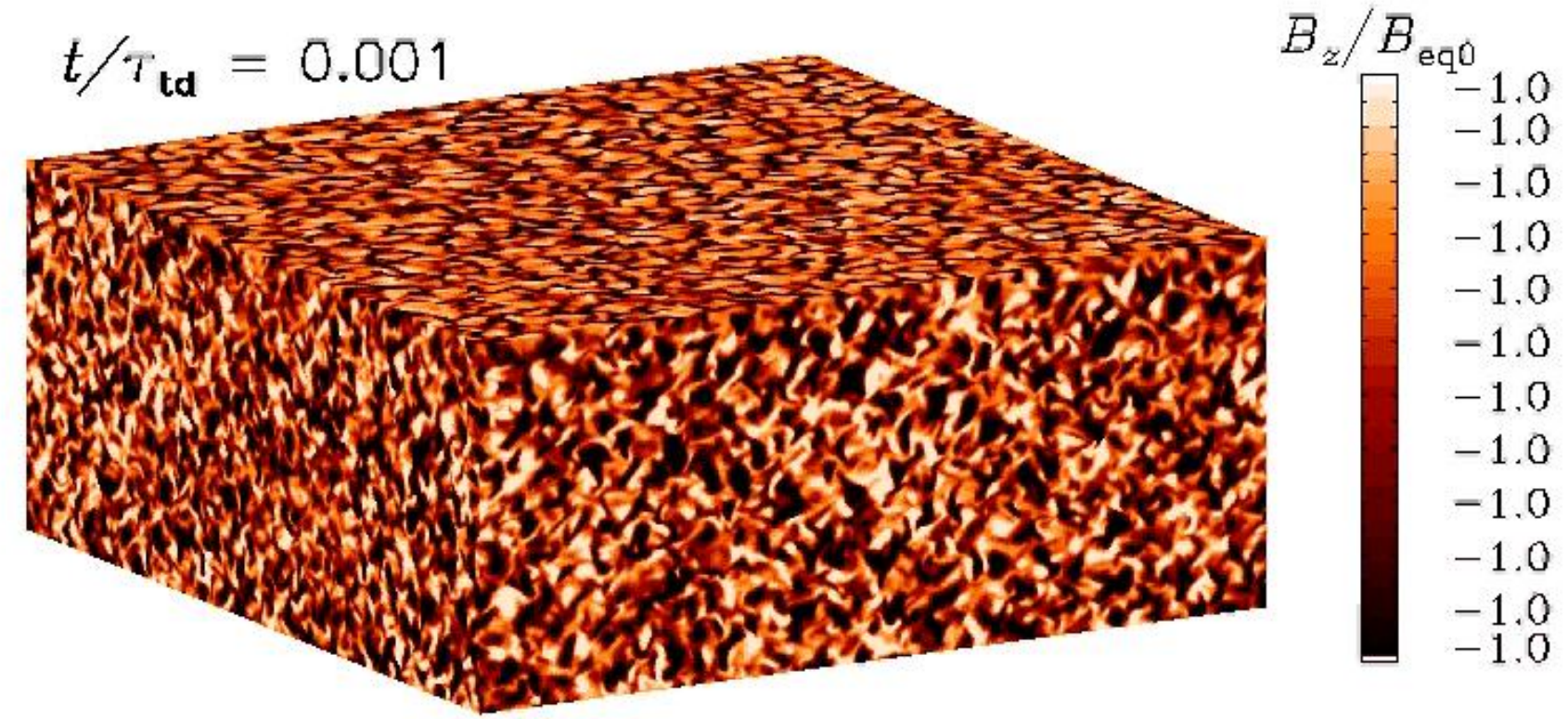

NEMPI is the Large-Scale Instability

A. Brandenburg, O. Gressel, S. Jabbari, N. Kleeorin, I. Rogachevskii,
Astron. Astrophys. 562, A53 (2014).

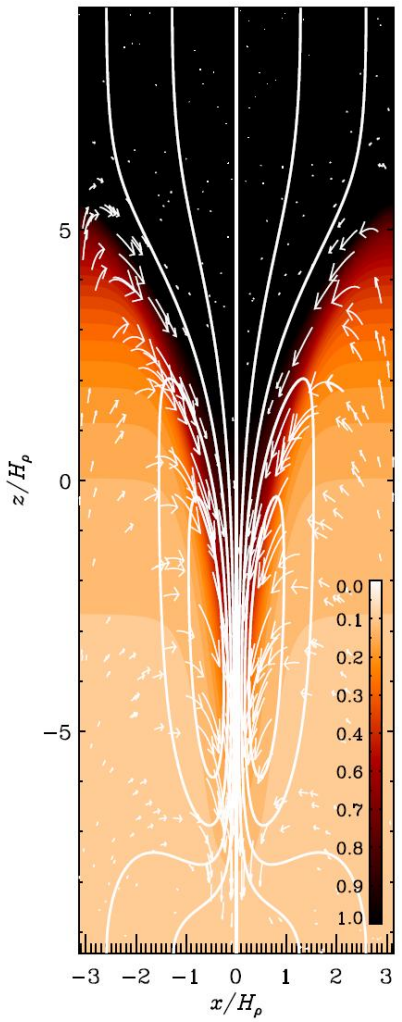

Fig. 5. $\overline{B}_z/B_{\rm eq}$ together with field lines and flow vectors from MFS, for Run Bv05/33 with $B_0/B_{\rm eq0} = 0.05$. The flow speed varies from $-0.27u_{\rm rms}$ (downward) to $0.08u_{\rm rms}$ (upward).

1. A local increase of the magnetic field causes a decrease of the negative effective magnetic pressure.
2. This is compensated for by enhanced gas pressure, leading to enhanced gas density, so the gas is heavier than its surroundings and sinks.
3. This results in a positive feedback loop: downflow compresses the magnetic field, the effective magnetic pressure becomes more negative, gas pressure increases, so the density increases, and the downflow accelerates, and causes NEMPI.

$$P_{\rm tot} = \rho T + (1 - q_p)\frac{\overline{\mathbf{B}}^2}{2}$$

DNS: 3D Turbulent Convection

P. Käpylä, A. Brandenburg, N. Kleeorin, M. Käpylä, I. Rogachevskii,
MNRAS, 422, 2465-2473 (2012); Astron. Astrophys. 588, A150 (2016).

$$\frac{\partial \boldsymbol{A}}{\partial t} = \boldsymbol{U} \times \boldsymbol{B} - \eta \mu_0 \boldsymbol{J},$$
$$\frac{D \ln \rho}{Dt} = -\boldsymbol{\nabla} \cdot \boldsymbol{U},$$
$$\frac{D\boldsymbol{U}}{Dt} = -\frac{1}{\rho}\boldsymbol{\nabla} p + \boldsymbol{g} + \frac{1}{\rho}\boldsymbol{J} \times \boldsymbol{B} + \frac{1}{\rho}\boldsymbol{\nabla} \cdot 2\nu\rho\mathbf{S},$$
$$\frac{De}{Dt} = -\frac{p}{\rho}\boldsymbol{\nabla} \cdot \boldsymbol{U} + \frac{1}{\rho}\boldsymbol{\nabla} \cdot K\boldsymbol{\nabla} T + 2\nu\mathbf{S}^2 + \frac{\mu_0 \eta}{\rho}\boldsymbol{J}^2,$$

$$\boldsymbol{B} = \boldsymbol{B}_0 + \boldsymbol{\nabla} \times \boldsymbol{A}$$

$$\mathrm{Re} = \frac{u_{rms}\, d}{2\pi\, \nu} = 40 - 100\,,$$

$$\mathrm{Rm} = \frac{u_{rms}\, d}{2\pi\, \eta} = 10 - 50\,,$$

$L_x = L_y = 5L_z = 5d;$ $(L_x = 10d)$ $\quad \frac{\rho_{bot}}{\rho_{top}} = 300;$

BOUNDARY CONDITIONS:

$U_z = 0, \quad \nabla_z U_x = \nabla_z U_y = 0$
$B_z \neq 0, \quad B_x = B_y = 0$

BOUNDARY CONDITIONS:

1).The horizontal boundaries are periodic.
2). We keep the temperature fixed at the top and bottom boundaries.
3) For the velocity we apply impenetrable, stress-free conditions.
4). For the magnetic field we use vertical field conditions.

Effective Magnetic Pressure is Negative in DNS with Turbulent Convection: but no NEMPI

P. Käpylä, A. Brandenburg, N. Kleeorin, M. Käpylä, I. Rogachevskii,
MNRAS, 422, 2465-2473 (2012); Astron. Astrophys. 588, A150 (2016).

$$\mathbf{F}^{\rm eff} = -\frac{1}{2}\nabla(1-q_p)\bar{\mathbf{B}}^2 + (\bar{\mathbf{B}}\cdot\nabla)(1-q_s)\bar{\mathbf{B}}$$

We perform horizontal averages which show a strong dependence on height.

We also perform time averaging in order to improve the statistics.

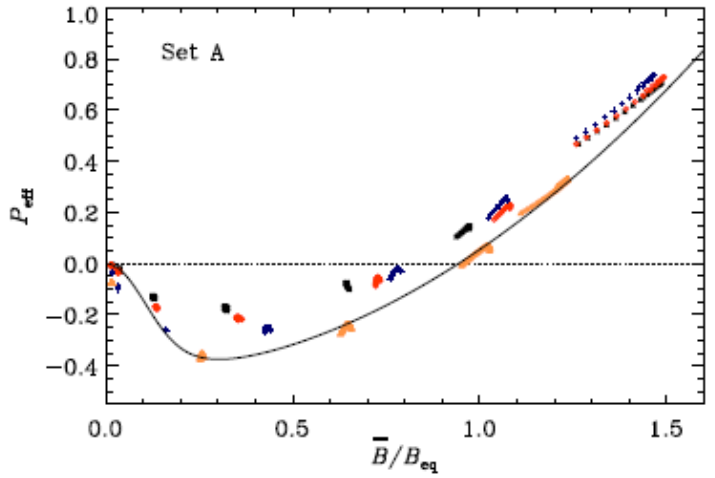

Figure 2. Effective magnetic pressure as a function of the mean magnetic field from weakly stratified Runs A1–A29 with an imposed horizontal field $\boldsymbol{B}_0 = B_0\hat{\boldsymbol{x}}$. The black stars, red diamonds, blue crosses, and yellow triangles denote simulations with Rm $\approx$ 10, 20, 50, and 70, respectively. We omit points near the boundaries at $z/d < 0.35$ and $z/d > 0.65$. The dashed and dotted lines correspond to approximate fits determined by Eq. (30), with $q_{p0} = 35$ and $B_p = 0.2B_{\rm eq}$, respectively.

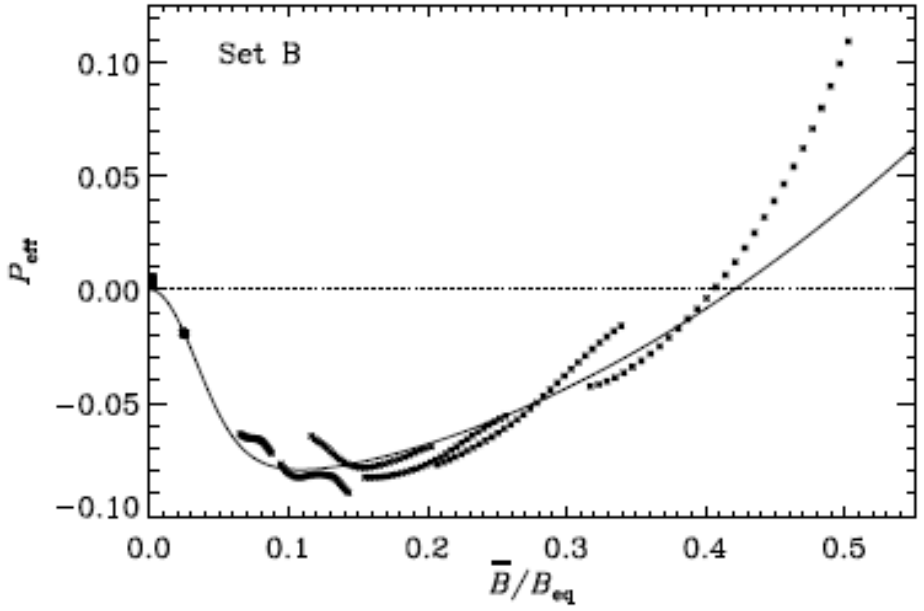

Figure 3. Same as Figure 2 but for Runs B1–B8 for Rm = 40–50. The solid line corresponds to a fit with $q_{\rm p0} = 70$ and $B_{\rm p} = 0.063B_{\rm eq}$

Mechanism of Large-Scale MHD-Instability

Let us consider an isolated flux tube of magnetic field lines. If the flux tube is lighter than the surrounding fluid, it moves upwards. The reason for continued upward floating of the magnetic flux tube is as follows.

The decrease of the magnetic field inside the ascending tube is due to its expansion.

This is accompanied by an increase of the magnetic pressure inside the tube. The latter is caused by the negative effective mean magnetic pressure.

The decrease of the magnetic field inside the tube results in a decrease of the fluid density and causes a buoyancy of the magnetic flux tube, i.e., the excitation of the large-scale instability.

The instability causes the formation of magnetic structures. The energy for this instability is supplied by the small-scale turbulence. In contrast, the free energy in Parker's magnetic buoyancy instability, is drawn from the gravitational field.

Growth Rate of Large-Scale MHD-Instability in Turbulent convection

Horizontal Magnetic Field

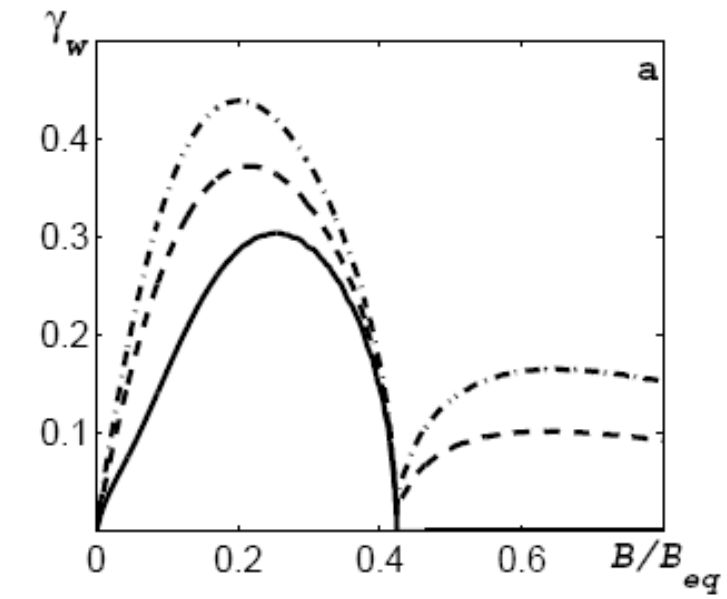

Vertical Magnetic Field

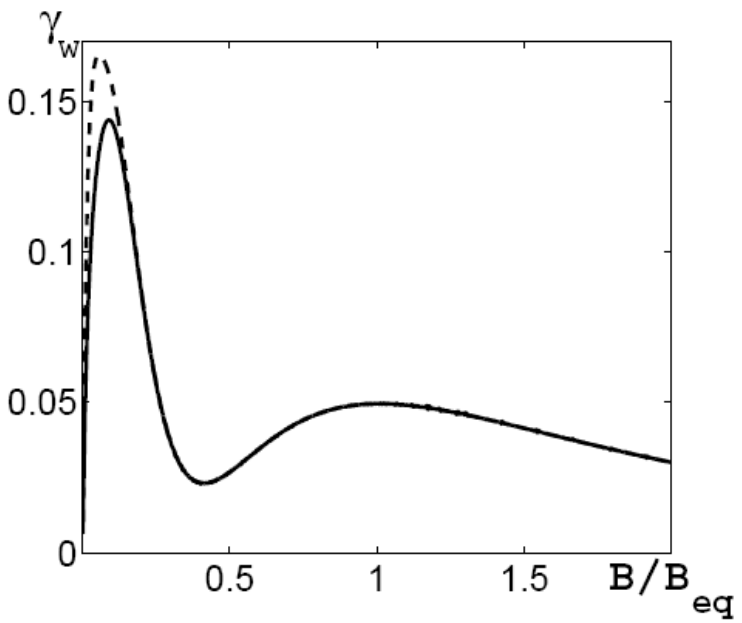

Large-Scale MHD-Instability

Let us estimate the growth rate of this instability. Neglecting dissipative processes for simplicity's sake, we shall retain only the Archimedes force in the momentum equation of the magnetic flux tube

$$\frac{d^2\zeta}{dt^2} = -\left(\frac{C_A}{C_s}\right)^2 \frac{gQ_p(L_B - L_\rho)}{L_B L_\rho}\zeta \ ,$$

where $C_A = \bar{B}_a/\sqrt{\mu\rho_a}$ is the Alfven velocity. The growth rate of this instability is given by

$$\gamma \simeq \frac{C_A}{L_\rho}\left[Q_p\left(\frac{L_\rho}{L_B} - 1\right)\right]^{1/2} \ .$$

Here $L_\rho \simeq C_s^2/g$.

Parameters (top of Solar Convective Zone)

In the upper part of the convective zone, at depth depth $H \sim 10^9$ cm,

the magnetic Reynolds number $\mathrm{Rm} \sim 3 \times 10^7$,

the maximum scale of turbulent motions $l_0 \sim 2.8 \times 10^8$ cm,

the characteristic turbulent velocity in the maximum scale l_0 of turbulent motions $u_0 \sim 10^4$ cm s^{-1},

the turbulent magnetic diffusion $\eta_T \sim 10^{12}$ cm^2 s^{-1},

the equipartition mean magnetic field $\bar{B}_{\mathrm{eq}} = 700$ G.

the characteristic time of developing of the instability $T \sim 1.2$ days; the turbulent diffusion time $T_D \sim 12$ days; the critical magnetic field for the instability $\bar{B}_{\mathrm{cr}} = 0.03 \bar{B}_{\mathrm{eq}}$.

Parameters (bottom of CZ)

The solar convective zone

At the base of the convective zone (at depth $H \sim 2 \times 10^{10}$ cm),

the magnetic Reynolds number $\mathrm{Rm} = l_0 u_0/\eta \sim 2 \cdot 10^9$,

the maximum scale of turbulent motions $l_0 \sim 8 \times 10^9$ cm,

the characteristic turbulent velocity $u_0 \sim 2 \times 10^3$ cm s^{-1},

the turbulent magnetic diffusion $\eta_T \sim 5.3 \times 10^{12}$ cm^{2}s^{-1},

the equipartition mean magnetic field $\bar{B}_{\mathrm{eq}} = 3000$ G.

the characteristic time of developing of the instability $T \sim 1$ year; the turbulent diffusion time $T_D \sim 3$ years; the critical magnetic field for the instability $\bar{B}_{\mathrm{cr}} = 0.1 \bar{B}_{\mathrm{eq}}$.

Summary

- Generation of magnetic fluctuations in a turbulence with large plasma beta results in a strong reduction of the large-scale magnetic pressure, so that effective magnetic pressure (sum of turbulent and non-turbulent contributions) can be negative.
- This causes excitation of negative effective magnetic pressure instability (NEMPI) and formation of the large-scale bipolar magnetic structures which are reminiscent Active Regions.

THE END